

## MOLECULAR TARGETS AS POTENTIAL PI3K $\alpha$ INHIBITORS AGAINST AGGRESSIVE METASTATIC DUCTAL AND LOBULAR CARCINOMA

ARPITH MATHEW<sup>1</sup>, SUBHAM DAS<sup>1</sup>, LATE ALEX JOSEPH<sup>1</sup>, SUMIT RAOSAHEB BIRANGAL<sup>1</sup>, JANE MATHEW<sup>2\*</sup>

<sup>1</sup>Department of Pharmaceutical Chemistry, Manipal College of Pharmaceutical Sciences, Manipal Academy of Higher Education, Manipal, Karnataka-576104, India. <sup>2</sup>Department of Pharmaceutical Chemistry, NGS Institute of Pharmaceutical Sciences, Nitte (Deemed to be University), Paneer, Deralakatte, Karnataka-575018, India

\*Corresponding author: Jane Mathew; Email: [janej@nitte.edu.in](mailto:janej@nitte.edu.in)

Received: 20 May 2024, Revised and Accepted: 17 Jul 2024

### ABSTRACT

**Objective:** This study aimed to identify active compounds among existing molecules by drug repositioning as potential hits of Phosphoinositide 3-Kinase (PI3K $\alpha$ ) inhibitors. FDA-approved ligands were docked using structure-based *in silico* screening, and the top ten molecules based on docking score were studied for their *in silico* pharmacokinetic and ligand-receptor interactions.

**Methods:** FDA-approved ligands were docked with the protein PI3K $\alpha$  enzyme (PDP ID: 4JPS) and were checked for their molecular interactions and docking scores using the GLIDE program of Schrödinger software. The top 10 ligands were subjected to ADMET and MMGBSA studies to predict pharmacokinetic properties and binding affinity. The best two molecules and the standard alpelisib were subjected to Molecular dynamics with 100 nsec simulation time to deduce interaction at the atomic level.

**Results:** Two molecules, ZINC00003794794 (Mitoxantrone) and ZINC00004098633 (Polydatin), were found to be promising based on docking score, ligand interaction diagram, and MMGBSA scores of -13.084 and -11.364 and -75.38 and -58.88 respectively and were in a comparable range to the standard alpelisib. These two molecules were then subjected to Induced Fit Docking (IFD) and molecular dynamics to better understand protein stability and inhibitor activity in physiological conditions. The IFD values of these molecules were very close to the standard, and the residues of the best poses coincided with the desired residues, such as V851, S854, and Q859, seen in the alpelisib.

**Conclusion:** However, further *in vitro* and *in vivo* screening is needed to confirm the PI3K $\alpha$  inhibitory activity of these ligands, which could serve as promising lead molecules in treating TNBC with fewer side effects compared to existing drugs.

**Keywords:** Drug repurposing, TNBC, PI3K $\alpha$ , Molecular docking and dynamics

© 2024 The Authors. Published by Innovare Academic Sciences Pvt Ltd. This is an open access article under the CC BY license (<https://creativecommons.org/licenses/by/4.0/>) DOI: <https://dx.doi.org/10.22159/ijap.2024v16i5.51514> Journal homepage: <https://innovareacademics.in/journals/index.php/ijap>

### INTRODUCTION

Breast cancer accounts for the highest number of cases reported by WHO, with about 2.26 million cases and deaths reaching 685,000 recorded in the year 2020 [1-3]. In breast cancer hormone therapy, it requires hormone receptors Estrogen (ER) and Progesterone (PR) and HER2 (Human Epidermal Growth Factor-2) expression to be effective, but in the case of Triple Negative Breast Cancer (TNBC), these receptors are not expressed, and the prognosis of patients with TNBC is poor and is more aggressive than other types of breast cancer [4].

TNBC accounts for almost 15% of the total breast cancer cases and is also linked to poor clinical outcomes. TNBC usually affects women under the age of 40 years and those who have genetic aberrations like BRCA1 or BRCA2 mutation [5, 6]. TNBC being triple negative, the usual drug therapies like abemaciclib given for hormone-positive breast cancer or trastuzumab, a monoclonal antibody used as an anti-HER2 agent but cannot be considered as targeted TNBC therapies [5-8].

In the carcinogenesis of the breast, PI3K alterations are the major pathway, and there is an interdependent connection between the PI3K enzyme, protein kinase B (AKT), and mTOR (Mammalian Target of Rapamycin) receptor, which together form a distinctive pathway. The PI3K/AKT/mTOR pathway, when exposed to certain factors like receptor tyrosine kinases and G-Protein Coupled Receptors, can lead to uncontrolled cell growth and cell division, leading to cancer [9, 10]. It is initiated by the formation of phosphoinositol trisphosphate (PIP3) from Phosphoinositol bisphosphate (PIP2); the PIP3 then picks up the protein kinase AKT, which is activated by the phosphorylation of mTORC2 (mTOR Complex 2). The stimulated AKT leads to the activation of other target proteins like FOXO (Forkhead Box O) and TSC2 (Tuberous Sclerosis Complex 2), which are the main components that form the known cancer cell properties [7-12]. The mutations in the PI3K pathway and

its downstream regulators tend to be the major factor in TNBC. PI3K $\alpha$  is mainly composed of two main subunits one is the catalytic subunit (P 110 $\alpha$ ) and the regulatory subunit (p 85 $\alpha$ ) [13]. The p85 $\alpha$  subunit includes alternative splicing comprising (p50a, p55a, and p85a) whose function is controlled by the PI3K1 gene [14].

Drug repurposing helps us find drug molecules that are already approved but with a new possible pharmacological action by using artificial advancements and artificial intelligence. The benefit of this approach is that it skips the processes, financial load, and time involved in getting a new drug molecule approved [15].

Molecular dynamics is an important component in drug discovery which is calculated by calculating the bonded and non-bonded forces acting on each atom and combined with quantum mechanics together, forming a force field; this force field is further used to calculate the position of the atoms by analyzing the lengths and dihedral angles of these atoms as experienced in reality by these molecules as MD is simulated based on normal body conditions [16, 17].

Alpelisib is the only PI3K $\alpha$  selective drug in the market sold under the brand name Piqray. Clinical reports mention a few drawbacks to its monotherapy. Hyperglycemia is a major side effect due to both the absorption and release of insulin and has not shown good efficacy against TNBC even though PI3K aberrations were seen, hence raising the need to find better drugs targeting this pathway and novel lead compounds for the treatment of this aggressive TNBC [18, 19].

### MATERIALS AND METHODS

#### In silico studies

The computational simulations were performed on Schrödinger software Maestro version 11.7.012, Release 2018-3, platform Linux-x86 64.

## Receptor

Protein PI3K $\alpha$  selective enzyme (PDB ID: 4JPS) was chosen for docking from the protein data bank and is composed of two chains, A and B, having a sequence length of 1074 and 293, respectively. The resolution of the protein is 2.20Å, has an observed R-value of 0.206, and is found in *Homo sapiens*. It contains a cocrystallized ligand alpelisib having the ID: 1LT, which is present on chain a of the protein [20]. Alpelisib is a selective inhibitor for the p110 $\alpha$  subunit used in various types of breasts and gastric cancer.

## Protein preparation, site map analysis, receptor grid generation

In Maestro, the protein is prepared using a protein preparation wizard in which the missing hydrogens, side chains, and side loops are added using the prime tool in Maestro. The Protein is then optimized by altering the spatial bonds of the hydrogen. The unwanted water molecules were removed, and the protein was minimized using the force field OPLS3E [21, 22].

The minimized protein was then split into ligands, waters, and others. Site Map analysis was performed on the apoprotein to find the suitable pocket for binding the ligand on the receptor. The best site based on the site score and the D score (druggability score) was compared with the position of the co-crystallized ligand, and chain B was deleted.

The Receptor Grid is generated using the Glide tool. The Van Der Waal radius factors were left at default; that is, the scaling factor was 1.0, and the partial charge cut-off, which considers the non-polar positions of the protein, was kept at 0.25. The size of the grid box was kept at default. The coordinates of the box: X=-1.3, Y=-9.36, Z= 16.53.

## Ligand preparation

FDA-approved ligands 1615 were downloaded from the Zinc database. These ligands were prepared using the LigPrep program (Epik tool). The ligands were set to default pH 7.0 $\pm$ 2.0, and under the stereoisomers tab, determine chirality from the 3D structure was ticked and generated at most 1 per ligand. LigPrep is required to generate energy-minimizing structures and correct mistakes that might have occurred due to computational errors.

## Molecular docking

The program used for molecular docking is Grid-Based Ligand Docking with Energetics (GLIDE). In molecular docking, the receptor is rigid, while the ligands are flexible and checked for various poses to find the best conformation and orientation of the ligand [23]. The affinity of the ligand-receptor complex is given by a scoring function that focuses on finding a global extremum of the value by finding the ideal binding mode of the ligand [24].

The ligands from LigPrep are docked onto the generated receptor grid. The initial precision is set to High Throughput Virtual Screening (HTVS), and the ligands are arranged based on their Docking score. The top 500 compounds are further subjected to Standard Precision (SP), which is slightly more refined and precise than HTVS. The top 100 compounds from SP are then subjected to Extra Precision (XP), which utilizes a more complex but more accurate and thorough scoring function that sorts the ligands semi-quantitatively based on their binding to the receptor [25].

The XP values are preferred for further studies because the scores obtained are a more complex scoring algorithm and are "harder" than those obtained from HTVS or SP and also take into consideration the shape formed by the ligand-receptor complex, and this helps to eliminate the false positive results obtained from SP.

The docking was validated by calculating the Root mean Square (RMS) of the co-crystallized ligand experimentally determined by X-ray diffraction with the same ligand generated after XP. The ligands were first aligned using quick align, and the Superposition task was selected. The RMS value was computed, and the results are shown in table 1. The interactions of the ligands with the amino acid residues of the XP minimized protein are presented in table 2.

## ADMET

ADMET was performed using QikProp, where the top 10 molecules based on XP docking glide score were selected, and the

information regarding the physicochemical properties of the ligands such as the polar surface area, logarithmic values, Lipinski's rule of five, such as molecular weight, Hydrogen Bond Donors and Hydrogen bond Acceptors was calculated, and the results are shown in table 3 and 4.

## MM/GBSA

The Prime tool in maestro performs molecular Mechanics with Generalized Born and Surface Area. The molecules from ADMET are further selected along with the XP minimized protein, solvation model employed is VSGB and force field OPLS3E.

The free energy binding between ligand and receptor was calculated by finding the individual free energies of the protein-ligand complex, the free energy of protein, and the free energy of the ligand. Internal, electrostatic, and van der Waal energies are required to calculate the free energy, and their respective polar and non-polar free energies are required [26]. The results are depicted in table 1.

## Induced fit docking

The molecules are subjected to induced fit docking where the receptor, as well as the ligand, are flexible. The docking is performed by the Glide tool, and the refinement is performed by the Prime tool. The first step involves a relaxed docking technique using van der Waal scaling, and then, based on the residues, a minimization is carried out for each ligand that considers the different positions and orientations of each ligand as it forms ligand-receptor complexes. The last step is docking the ligand to the induced-fit protein using the Glide tool and XP precision [27]. The protein selected is the initial minimized protein with the co-crystallized ligand, and the ligands from MM/GBSA are selected for induced fit docking. All the parameters are kept at default except for glide redocking, which was changed to XP, and 'write XP descriptors' was ticked, and the program was run.

## Molecular dynamics

Dynamics is used to determine the position and movement (velocity) of atoms in a protein after each femtosecond by using Newtonian laws of motion, which consider the various forces acting on each atom [28, 29]. Force fields are used to calculate the potential energies of the atoms, which use molecular mechanics.

The first step in molecular dynamics is to form a ligand-protein complex by merging the ligand with the protein. The system builder task was selected from the Desmond application, and the complex was engulfed with water molecules using the predefined solvent water model, simple point charge (SPC), which is original and refined. The boundary parameters were kept at the default settings; the box shape was orthorhombic, the method for box size calculation was buffer, and the box dimensions were kept equally from all points, that is, 10Å distance and 90 angles. The volume was minimized by clicking minimize the volume and ticking the show boundary box. The project was run, and the system build model was developed and presented in the workspace. The next step is minimization from the Desmond application, where the system build model was loaded from the workspace, the simulation time was set, and the job was run. The last step is selecting the molecular dynamics task from the Desmond application and loading the minimized model from the workspace. The stimulation time was set to 100ns at the start and approximately 1000 frames. Under the ensemble class, NPT was chosen and kept at the default temperature (300K) and default pressure (1.01325 bar) [30].

## RESULTS

The protein selected for the study is a PI3K $\alpha$  enzyme selected from the protein data bank having a PDB ID: 4JPS. The missing parts of the structure were added using the prime tool and Prot Assign at the default pH of 7.0 $\pm$ 2.0. The structure was optimized and then minimized in Maestro. The 2,531 prepared ligands were obtained after LigPrep and were docked onto the receptor grid of 4JPS.

Structure-based virtual screening was executed on the receptor grid, which was generated around the co-crystallized ligand. The glide tool docked the prepared ligands onto the receptor within the box.

First, HTVS was performed for all the prepared ligands; then, for the top 500 SP and the top 100 compounds, XP was performed. The RMSD to input ligand geometries option was ticked in the output function of ligand docking, and hence we got the RMSD scores.

The validation was done by selecting the co-crystallized ligand from the protein taken from the data bank and the XP obtained pose of the co-crystallized ligand. The RMS score was 0.6097, which is less than 2.000, hence validating the docking protocol.

**Table 1: Top 10 compounds after XP docking with their chemical structure, docking, and MM/GBSA score**

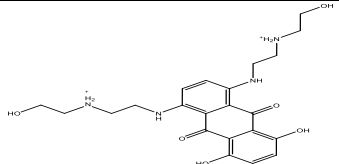
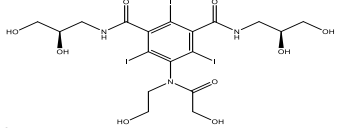
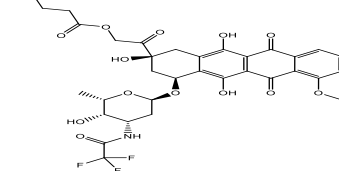
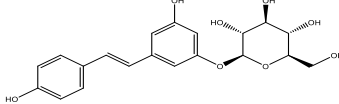
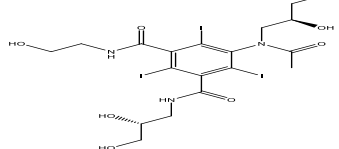
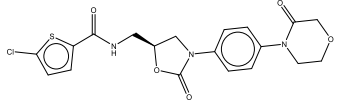
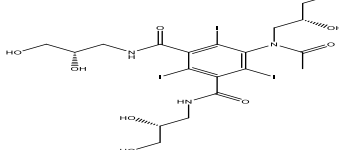
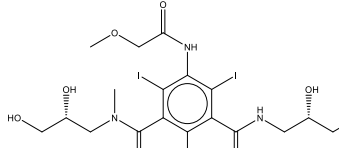
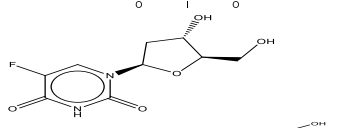
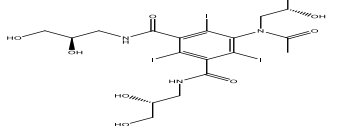
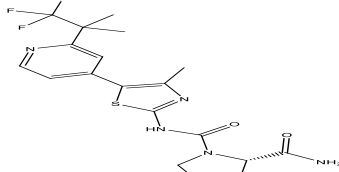
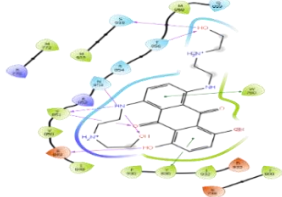
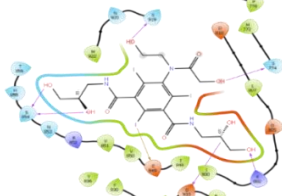
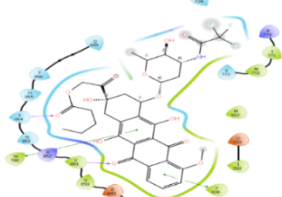
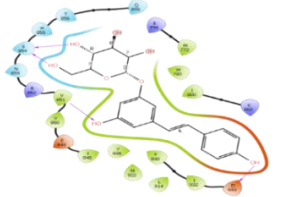
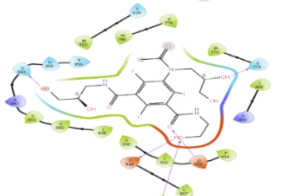
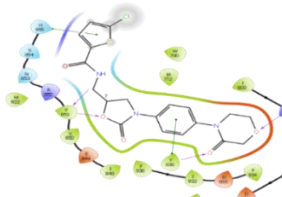

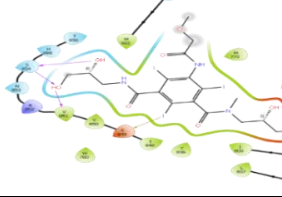
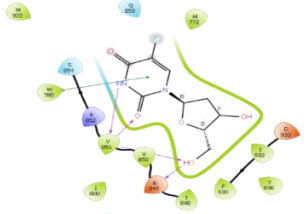
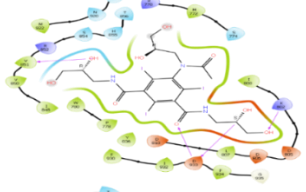
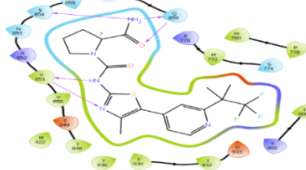
Compound	Chemical structure	Docking score	MM GBSA (kcal mol <sup>-1</sup> )
ZINC000003794794 (Mitoxantrone)		-13.084	-75.38
ZINC000008143866		-11.449	-34.09
ZINC000049783788 (Valrubicin)		-11.393	-60.19
ZINC000004098633 (Polydatin)		-11.364	-58.88
ZINC000085540219 (Ioxilan)		-11.099	-27.79
ZINC000003964126 (rivaroxaban)		-10.959	-44.27
ZINC000003830946		-10.945	-21.27
ZINC000003830958		-10.923	-31.27
ZINC000003813010 (Floxuridine)		-10.825	-24.66
ZINC000008035377		-10.736	-26.70
Alpelisib		-12.607	-72.37

Table 2: Ligand interaction with amino acid residues of the top 10 compounds obtained from XP with the protein

Compound	Ligand-Interaction diagram	Amino acid residues
ZINC000003794794		H-Bond: N853, S919, T856, V851(2), E849 Pi-Pi stacking: Y836, W780 Charged(-ve):E849, D933, E798 Charged(+ve):R852, R770 Polar: S919, S854, T856, N853, Q859 Hydrophobic: V851,V850, I848, I932, Y836, I800, M772, W780, M922, F930, M858
ZINC000008143866		H-Bond: S854 (2), S919, S774, K802, D933. Halogen Bond: E849 Charged(-ve): D933, D810, D805, E849 Charged(+ve):R852, K802 Polar: : N920, S919, S854, H855, T856, S774, N853 Hydrophobic: V851,V850, I848, I932, Y836, I800, M772, W780, M922, P778, F930, F934, L807
ZINC000049783788		H-Bonds: S854, V851 Pi-Pi stacking: W780, Y836 Charged(-ve): D933, E849, E798 Charged(+ve): R770, R852 Polar: N853, S854, H855, T856, Q859, Q728, S773 Hydrophobic: V851,V850, I848, I932, Y836, I932, I800, M772, W780, M922.
ZINC000004098633		H-Bonds: S854(2), V851, D933 Charged(-ve): D933, E849 Charged (+ve): R852, K802,R770 Polar: N853, S854, H855, T856, Q859 Hydrophobic: V851,V850, I848, F930, L814, I932, Y836,I932,L807,I800,M772 W780,M922
ZINC000085540219		H-Bond: S854, D810, D933, Y836, S774 Charged(-ve):D810, D933 Charged(+ve): K802, R852 Polar: S919, S774, H855, T856, S854 Hydrophobic: V851,V850, I848, I932, Y836, I800, M772, P778, W780, M922, F930, L807, C838, F934, L814
ZINC000003964126		H-Bond: V851(2), Y836, K802 Pi-Pi stacking: H855, Y836 Charged(-ve): E849, D933, D810 Charged(+ve):K802, R852 Polar: N853, H855, S854 Hydrophobic: V851, V850, I848, I932, Y836, I800, M772, W780, M922, L807, F934, F930, L814
ZINC000003830946		H-Bond: S854(2), K802, D933, Y836, Halogen Bond: E849 Charged (-ve): D810,D933, E849 Charged (+ve): R852,K802 Polar: N853, S854, H855, T856, S919, S774, Hydrophobic: V851,V850, I848, F930, C838,L814, Y836,I932,F934,L807,I800,M772,P778,W780,M922
ZINC000003830958		H-Bond: S854(2), V851, K802, D933(2) Halogen Bond: E849 Charged(-ve): E849, D810, D933 Charged(+ve):K802, R852 Polar: S919, N853, H855, T856, S854 Hydrophobic: V851, V850, I848, I932, Y836, I800, M772, W780, M922, L807, F934

Compound	Ligand-Interaction diagram	Amino acid residues
ZINC000003813010		H-Bond: V851(3), E849 Pi-Pi stacking: W780 Charged(-ve): D933, E849 Charged(+ve): R852 Polar: S854, Q859 Hydrophobic: V851, V850, I848, I932, Y836, I800, M772, W780, M922, F930
ZINC000008035377		H-Bond: V851, D933 (2), K802. Charged(-ve): D933, D810, D806, D805 Charged(+ve): R770, R852, K802 Polar: N920, S919, S854, H855, T856, S774 Hydrophobic: V851, V850, I848, I932, Y836, I800, M772, W780, M922, P778, F930, F934, L807 Glycine: G935
Alpelisib		H-Bond: S854, Q859(2), V851(2) Charged(-ve): D933, E849 Charged(+ve): K802, R770, R852 Polar: N853, S854, H855, T856, Q859, S774 Hydrophobic: V851, V850, I848, I932, Y836, I800, M772, W780, M922, F930, P778

The docking scores of the top 10 molecules from XP docking were in the range of -13.084 to -10.736 and the MM/GBSA scores were in the range of -75.38 to -21.27 kcal/mol, the standard Alpelisib, which is the co-crystallized ligand showed a docking score value of -12.607 and an MM/GBSA score of -72.37 kcal/mol. Alpelisib showed H-bonding interactions with the residues S854 (H-bond interaction at the nitrogen of the amide group) and V851 (2 H-bond interactions, one at the secondary amine and the other on the nitrogen of the thiazole ring). The best ligand in this study (Zinc ID:

ZINC000003794794) showed better docking and MM/GBSA scores than the standard, as shown in table 1.

ADMET analysis: Five compounds deferred from the rule of five in less than 2 parameters, as shown in table 3. Following the analysis, seven compounds showed no related cardiac toxicity by blocking the HERG channel since their QPlog HERG value is greater than -5.0 [31-34]. The cell gut permeability QPPCaco values are less than 500, and QPlogBB values are negative, indicating that all ten compounds will not cross BBB and thus would not cause the undesired CNS effects, as shown in table 4.

Table 3: Lipinski's rule of 5 for the top 10 compounds

Compound code	Mol MW	Donor HB	Acceptor HB	Rule of 5	PSA	% HOA
ZINC000003794794	444.486	4.	9	1	186.680	10.94
ZINC000008143866	807.116	8	18	3	222.288	0.00
ZINC000049783788	723.653	3.	16	2	222.078	34.49
ZINC000004098633	390.389	6	10	1	145.747	39.40
ZINC000085540219	791.116	7	16	3	197.786	6.93
ZINC000003964126	435.881	1	10	0	117.107	84.87
ZINC000003830946	821.143	8	18	3	226.986	0.00
ZINC000003830958	791.116	6	16	3	182.677	14.92
ZINC000003813010	246.195	3	8	0	118.019	63.99
ZINC000008035377	821.143	8	18	3	222.419	0.00

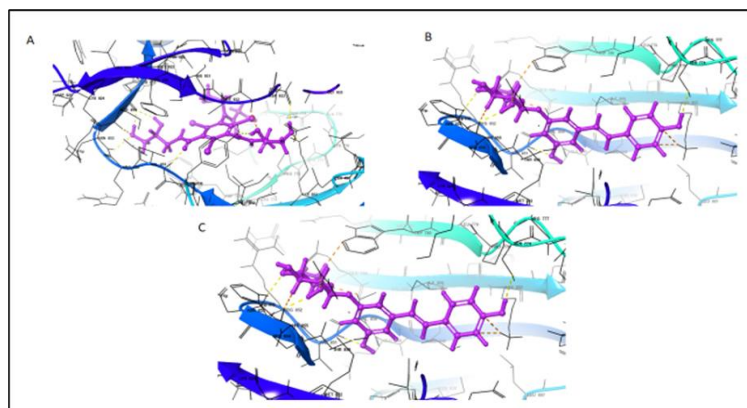
Table 4: ADMET properties of top 10 molecules

Compound code	QPlogkhsa	QPlogPo/w	QPlogS	QPlogHERG	QPPCaco	QPlogBB	QPPMDCK
ZINC000003794794	-0.410	0.133	-1.284	-7.239	0.611	-3.061	0.203
ZINC000008143866	-1.428	-1.592	-2.272	-4.788	5.361	-3.804	7.619
ZINC000049783788	-0.557	2.030	-4.855	-4.704	16.054	-3.065	51.136
ZINC000004098633	-0.754	0.115	-2.948	-6.079	24.107	-3.040	8.823
ZINC000085540219	-1.137	-0.576	-2.659	-4.519	17.461	-2.982	31.226
ZINC000003964126	-0.345	2.052	-4.859	-5.704	367.062	-0.905	728.060
ZINC000003830946	-1.343	-1.364	-2.472	-4.758	4.459	-3.870	6.621
ZINC000003830958	-1.159	-0.291	-2.933	-4.830	39.411	-2.659	73.870
ZINC000003813010	-0.783	-0.778	-1.427	-2.629	210.959	-0.829	162.695
ZINC000008035377	-1.385	-1.529	-2.515	-4.937	3.745	-4.099	4.468

#### Induced fit docking

IFD is a tool that takes into consideration the conformational changes that happen to a protein when a small drug molecule binds to it [27]. IFD was performed for two molecules (ZINC000003794794 and ZINC000004098633) and standard. The

IFD scores, along with a 3-D structure of their respective complexes of the two main compounds and the standard, is shown in fig. 1. The IFD values of the two molecules are very close to the standard, and the residues of the best poses are also coinciding with our desired residues such as V851, S854 and Q859 which are the residues seen in the alpelisib IFD.



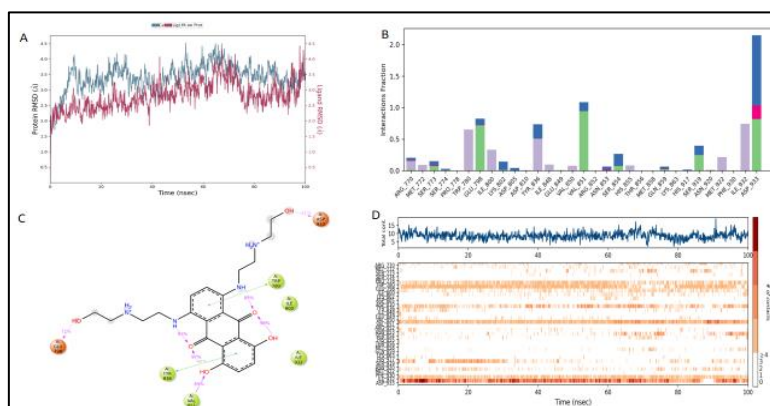
**Fig. 1:** 3D ligand interaction diagram of the top 2 molecules and the standard alpelisib along with their IFD score; A: ZINC000003794794 (2198.21), B: ZINC000004098633 (-2199.24), C: Alpelisib (-2198.71)

### Molecular dynamic simulations

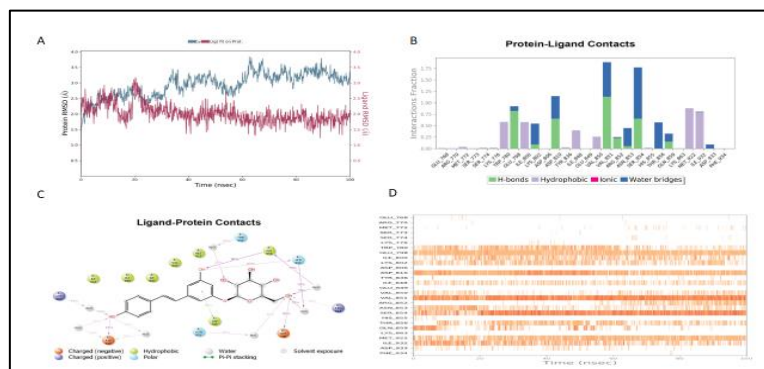
The selection of the compounds was based on XP dock scores, MM/GBSA scores, and ligand interaction diagram. The dynamics simulation was performed on ZINC000003794794 (Mitoxantrone), which had the highest dock score and MM/GBSA score in the study and was also higher than the standard. ZINC000004098633 (polydatin) had a comparable score in terms of dock score and MM/GBSA score to valrubicin, but the reason for selecting this molecule was that it had a higher IFD score and the number of amino acid interactions were higher and better suited for enzyme selectivity as compared to valrubicin. The molecular dynamics of ZINC000003794794 showed very stable interaction with D933,

which was also seen in polydatin, and the standard selected was alpelisib, which is also the co-crystal ligand of PI3K  $\alpha$  protein (4JPS), and the results obtained were compared.

The RMSD of the protein shown in fig. 2 lies between 1.5Å and approximately 4.3Å, which is in the acceptable fluctuation range. The promising factor in these dynamics reports, apart from the higher dock score and MM/GBSA score, is the relative stability of the receptor-ligand complex as we see both the C $\alpha$  and the lig fit prot almost on par with each other and also at some points overlapping can be noticed showing that the ligand can keep up with the conformational changes of the protein and is stable at the initial binding site.



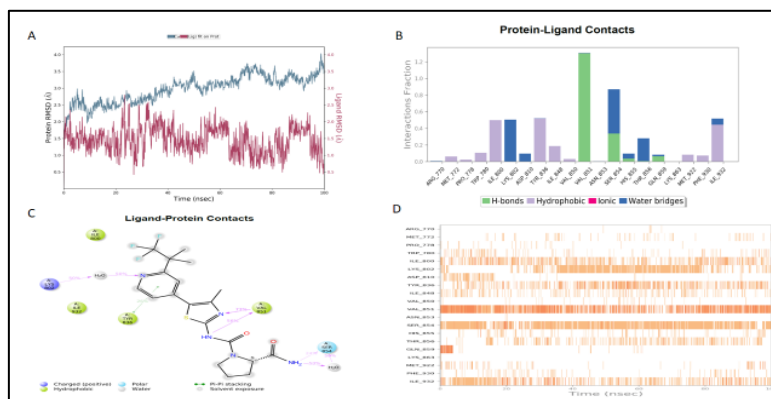
**Fig. 2:** ZINC000003794794 MD; A) RMSD plot of protein-ligand complex, B) Histogram of protein-ligand complexes, C) Diagram of protein-ligand contacts, D) Number of contacts and duration of contact with the protein



**Fig. 3:** ZINC000004098633 MD; A) RMSD plot of protein-ligand complex, B) Histogram of protein-ligand complexes, C) Diagram of protein-ligand contacts, D) Number of contacts and duration of contact with the protein

The RMSD of ZINC000004098633 in fig. 3 showed that the protein RMSD was seen to be between 2-3.5Å and the lig fit on prot was seen to be stable throughout the 100nsec simulation in the range of 2-2.5Å, no drastic difference is seen in both their ranges, meaning the

ligand was pretty stable within the complex. The RMSD of the protein is stable within the range of 2.0Å and 4.0Å, and the lig fit on prot is at a lower range of 0.5 Å and 2.5 Å, which is in the acceptable range, as shown in fig. 4.



**Fig. 4: Alpelisib MD; A) RMSD plot of protein-ligand complex, B) Histogram of protein-ligand complexes, C) Diagram of protein-ligand contacts, D) Number of contacts and duration of contact with the protein**

## DISCUSSION

The genetic dysregulation of the PI3K enzyme is one of the major causes of cancer, and it found that the  $\alpha$  subtype is majorly expressed in breast cancers, especially in TNBC [8]. PI3KCA is shown to have various mutations that either tend to repress the activity of the catalytic subunit P110 $\alpha$  by the regulatory subunit p85 or amplify the relationship between the catalytic subunit to the lipid membrane at E545K in exon 9 and H1047RK in exon 20 respectively [14]. With technological advancements and the development of *in silico* tools, possible lead molecules could be discovered that would bind well to our desired enzyme of interest, PI3K $\alpha$ , which was selected after extensive study of how the protein deregulates cell proliferation and loss of apoptosis in Triple Negative Breast Cancer.

The ligand interaction diagrams reflected the amino acid residues involved in binding the ligand with the protein. Of the ten molecules, the most common H-bonding residues were V851 and S854 and D933 and K802 residues but are comparatively lesser than the former residues shown in table 2. V851 is a valine hydrophobic residue, also known as the hinge residue, and S854 is a serine polar residue that is critical for  $\alpha$  selectivity to bind to the carbonyl group of the serine residue. D933 is a negatively charged aspartic acid residue, and K802 is a positively charged lysine residue. There are a few molecules that showed pi-pi stacking residue W780, which is tryptophan and is unique to the  $\alpha$  subunit, hence increasing its selectivity over the beta subunit of the residue and is preserved within the PI3K class of enzymes [33, 34]. Further studies were done with induced fit docking and molecular dynamics.

The best drug molecule in this study, Mitoxantrone, is an anti-neoplastic agent [35]. The molecular dynamics report of the ligand-protein contact diagrams of ZINC000003794794, as seen in fig. 2 shows that D933 and V851 are the two highest occurring interactions and are almost completely involved in the binding of the ligand and the protein throughout the 100 sec, although it is seen that the number of contacts with D933 is higher indicated by the darker shades of orange in the fourth diagram of fig. 2 and the histogram also shows a much higher interaction fraction. Val 851, on the other hand, shows a high percentage of contact of about 89% with the hydroxyl group of the ligand, confirming that it was almost completely part of the complex and is also reported in papers to be a critical residue for PI3K $\alpha$  selectivity [36]. T780, which forms a pi-pi stacking bond with the molecule, is reported to be an important interaction for  $\alpha$  selectivity, and the tryptophan amino acid is preserved within the PI3K class; hence, in the case of beta selectivity, T781 will be seen [33].

The next best drug that was selected in this study based on docking score, residue interaction, MMGBSA score, and IFD score was

polydatin. Polydatin is a polyphenolic compound derived mainly from the roots of *Polygonum cuspidatum* that is enriched with a plethora of pharmacological uses ranging from being an anti-oxidant, anti-diabetic, anticancer agent, and many more [32].

The molecular dynamics report of ZINC000004098633 showed protein-ligand contacts show that V851 is the major residue involved in the complex formation and the darker orange portion of diagram four along with the percentage of contact seen in diagram 3 of fig. 3. It is possible to say that the residue has a high number of contacts with the ligand almost completely the entire 100nsec. The other major interactions are seen with S854 after 20nsec with more contacts and D810 with a percentage contact of 65% with the molecule. The acceptable criteria for fluctuation is between 1-4 Å. The promising findings are that most residues taking part in the complex formation are considered crucial interactions for PI3K $\alpha$  activity, including M922 and I932 [37].

These molecules have no reports of hyperglycemia being a side effect like that seen in various papers about alpelisib [19]. The molecular dynamics of our top two drugs show much better results than our standard regarding their stability. The protein-ligand diagrams of alpelisib show that the major interactions are with V851 and S854, which have almost continuous contact with the ligand at higher contact points. The fourth diagram shows darker shades of orange. S854 shows H-bonds with the amino group as well as with the water molecule surrounding it and is also confirmed in the histogram, whereas the V851 has only H-bond formation with the thiazole ring and the secondary amine of alpelisib as shown in fig. 4. The MD of alpelisib showed larger conformational changes in the protein structure indicating that the complex was not very stable whereas the top 2 ligands showed minor conformational changes in the protein structure although more stable than the standard, indicating mitoxantrone and polydatin have better binding activity with the PI3K $\alpha$  receptor and could also provide better pharmacological response, in the case of this study a possible anti TNBC agent.

## CONCLUSION

The study aimed to find safer and more potent PI3K $\alpha$  inhibitors that could be used as possible agents against TNBC through drug repurposing of US-FDA drugs using *in silico* tools. A total of 1615 compounds were taken from the ZINC database to study docking. The top 10 molecules based on docking score were then selected, and their pharmacokinetic profile was studied. Further screening of ZINC000003794794 (Mitoxantrone) and ZINC000004098633 (Polydatin) based on docking score, MM/GBSA, and ligand-interaction diagram were subjected to induced fit docking and molecular dynamics. The results obtained from the computational

study prove to be promising step forward in obtaining potential candidates in treating this very aggressive form of breast cancer, but further *in vitro* and *in vivo* studies need to be carried out to study their cytotoxic activities against TNBC and its importance to do an enzyme selectivity test of these molecules to see the inhibitory activity of these molecules to the PI3K enzyme as well as against its subtypes to get a clearer picture of how these drugs would bind to the PI3K enzyme practically.

#### ACKNOWLEDGMENT

The authors thank the Manipal College of Pharmaceutical Sciences and Manipal Academy of Higher Education for providing support and research facilities and the Manipal-Schrodinger Centre for Molecular Simulations.

#### FUNDING

Nil

#### AUTHORS CONTRIBUTIONS

Arpith M: Conceptualization of idea, performing *insilico* studies, interpretation of data, draft preparation. Late Alex Joseph: Interpreting data, draft editing, supervision. S Das: Performing molecular dynamics interpretation of data. S R Birangal: Performed molecular dynamics and interpretation of data. Jane M: discussion, reviewing, draft preparation, and manuscript finalization.

#### CONFLICT OF INTERESTS

The authors have no conflict of interest.

#### REFERENCES

- Hanahan D, Weinberg RA. Hallmarks of cancer: the next generation. *Cell*. 2011;144(5):646-74. doi: [10.1016/j.cell.2011.02.013](https://doi.org/10.1016/j.cell.2011.02.013), PMID 21376230.
- Arnold M, Morgan E, Rungay H, Mafra A, Singh D, Laversanne M. Current and future burden of breast cancer: global statistics for 2020 and 2040. *Breast*. 2022;66:15-23. doi: [10.1016/j.breast.2022.08.010](https://doi.org/10.1016/j.breast.2022.08.010), PMID 36084384.
- Dwivedi U, Jain A, Ali Fb, Ali M. Evaluation of serum and salivary Ca-125 in breast cancer patients-an analytical study. *Asian J Pharm Clin Res*. 2023;16(4):97-9. doi: [10.22159/ajpcr.2023.v16i4.46864](https://doi.org/10.22159/ajpcr.2023.v16i4.46864).
- Sotiriou C, Pusztai L. Geneexpression signatures in breast cancer. *N Engl J Med*. 2009;360(8):790-8. doi: [10.1056/NEJMra0801289](https://doi.org/10.1056/NEJMra0801289).
- De Laurentiis M, Cianniello D, Caputo R, Stanzione B, Arpino G, Cinieri S. Treatment of triple negative breast cancer (TNBC): current options and future perspectives. *Cancer Treat Rev*. 2010;36Suppl 3:S80-6. doi: [10.1016/S0305-7372\(10\)70025-6](https://doi.org/10.1016/S0305-7372(10)70025-6), PMID 21129616.
- Zucca Matthes G, Urban C, Vallejo A. Anatomy of the nipple and breast ducts. *Gland Surg*. 2016;5(1):32-6. doi: [10.3978/j.issn.2227-684X.2015.05.10](https://doi.org/10.3978/j.issn.2227-684X.2015.05.10), PMID 26855906.
- Vernieri C, Milano M, Brambilla M, Mennitto A, Maggi C, Cona MS. Resistance mechanisms to anti-HER2 therapies in HER2-positive breast cancer: current knowledge new research directions and therapeutic perspectives. *Crit Rev Oncol Hematol*. 2019;139:53-66. doi: [10.1016/j.critrevonc.2019.05.001](https://doi.org/10.1016/j.critrevonc.2019.05.001), PMID 31112882.
- Costa RL, Han HS, Gradishar WJ. Targeting the PI3K/AKT/mTOR pathway in triple-negative breast cancer: a review. *Breast Cancer Res Treat*. 2018;169(3):397-406. doi: [10.1007/s10549-018-4697-y](https://doi.org/10.1007/s10549-018-4697-y), PMID 29417298.
- Leever SJ, Vanhaesebroeck B, Waterfield MD. Signalling through phosphoinositide 3-kinases: the lipids take centre stage. *Curr Opin Cell Biol*. 1999;11(2):219-25. doi: [10.1016/S0955-0674\(99\)80029-5](https://doi.org/10.1016/S0955-0674(99)80029-5), PMID 10209156.
- Ali YS, Mahdi MF, Razik BM. In silico evaluation of binding interaction and ADME properties of novel 5-(Thiophen-2-Yl)-1,3,4-oxadiazole-2-amine derivatives as antiproliferative agents. *Int J App Pharm*. 2023;15(1):141-6. doi: [10.22159/ijap.2023v15i1.46488](https://doi.org/10.22159/ijap.2023v15i1.46488).
- Sabbah DA, Hajjo R, Bardaweel SK, Zhong HA. Phosphatidylinositol 3-kinase (PI3K) inhibitors: a recent update on inhibitor design and clinical trials (2016-2020). *Expert Opin Ther Pat*. 2021;31(10):877-92. doi: [10.1080/13543776.2021.1924150](https://doi.org/10.1080/13543776.2021.1924150), PMID 33970742.
- Curigliano G, Shah RR. Safety and tolerability of phosphatidylinositol-3-Kinase (PI3K) inhibitors in oncology. *Drug Saf*. 2019;42(2):247-62. doi: [10.1007/s40264-018-0778-4](https://doi.org/10.1007/s40264-018-0778-4), PMID 30649751.
- Miricescu D, Totan A, Stanescu Spinu II, Badoiu SC, Stefani C, Greabu M. PI3K/AKT/mTOR signaling pathway in breast cancer: from molecular landscape to clinical aspects. *Int J Mol Sci*. 2020;22(1):1-24. doi: [10.3390/ijms22010173](https://doi.org/10.3390/ijms22010173), PMID 33375317.
- Hoxhaj G, Manning BD. The PI3K AKT network at the interface of oncogenic signalling and cancer metabolism. *Nat Rev Cancer*. 2020;20(2):74-88. doi: [10.1038/s41568-019-0216-7](https://doi.org/10.1038/s41568-019-0216-7), PMID 31686003.
- Yang J, Nie J, Ma X, Wei Y, Peng Y, Wei X. Targeting PI3K in cancer: mechanisms and advances in clinical trials 06. *J Biol Sci*. 2019;18(1):26. doi: [10.1186/s12943-019-0954-x](https://doi.org/10.1186/s12943-019-0954-x).
- Rodon J, Dienstmann R, Serra V, Tabernero J. Development of PI3K inhibitors: lessons learned from early clinical trials. *Nat Rev Clin Oncol*. 2013;10(3):143-53. doi: [10.1038/nrclinonc.2013.10](https://doi.org/10.1038/nrclinonc.2013.10), PMID 23400000.
- Racz A, Mihalovits LM, Bajusz D, Heberger K, Miranda Quintana RA. Molecular dynamics simulations and diversity selection by extended continuous similarity indices. *J Chem Inf Model*. 2022 Jul 25;62(14):3415-25. doi: [10.1021/acs.jcim.2c00433](https://doi.org/10.1021/acs.jcim.2c00433), PMID 35834424.
- Durrant JD, McCammon JA. Molecular dynamics simulations and drug discovery. *BMC Biol*. 2011;9(1):71. doi: [10.1186/1741-7007-9-71](https://doi.org/10.1186/1741-7007-9-71), PMID 22035460.
- Yu M, Chen J, Xu Z, Yang B, He Q, Luo P. Development and safety of PI3K inhibitors in cancer. *Arch Toxicol*. 2023;97(3):635-50. doi: [10.1007/s00204-023-03440-4](https://doi.org/10.1007/s00204-023-03440-4), PMID 36773078.
- Savas P, Lo LL, Luen SJ, Blackley EF, Callahan J, Moodie K. Alpelisib monotherapy for PI3K-altered pretreated advanced breast cancer: a Phase II study. *Cancer Discov*. 2022;12(9):2058-73. doi: [10.1158/2159-8290.CD-21-1696](https://doi.org/10.1158/2159-8290.CD-21-1696), PMID 35771551.
- Furet P, Guagnano V, Fairhurst RA, Imbach Weese P, Bruce I, Knapp M. Discovery of NVP-BYL719 a potent and selective phosphatidylinositol-3 kinase alpha inhibitor selected for clinical evaluation. *Bioorg Med Chem Lett*. 2013;23(13):3741-8. doi: [10.1016/j.bmcl.2013.05.007](https://doi.org/10.1016/j.bmcl.2013.05.007), PMID 23726034.
- Sastry GM, Adzhigirey M, Day T, Annabhimoju R, Sherman W. Protein and ligand preparation: parameters protocols and influence on virtual screening enrichments. *J Comput Aided Mol Des*. 2013;27(3):221-34. doi: [10.1007/s10822-013-9644-8](https://doi.org/10.1007/s10822-013-9644-8), PMID 23579614.
- Jayanthi K, Ahmed SS, Baqi MA, Afzal Azam M. Molecular docking dynamics of selected benzylidene aminophenyl acetamides as TMK inhibitors using high throughput virtual screening (HTVS). *Int J App Pharm*. 2024;16(3):290-97. doi: [10.22159/ijap.2024v16i3.50023](https://doi.org/10.22159/ijap.2024v16i3.50023).
- Friesner RA, Banks JL, Murphy RB, Halgren TA, Klicic JJ, Mainz DT. Glide: a new approach for rapid accurate docking and scoring. 1. Method and assessment of docking accuracy. *J Med Chem*. 2004 Mar;47(7):1739-49. doi: [10.1021/jm0306430](https://doi.org/10.1021/jm0306430), PMID 15027865.
- Jain AN. Scoring functions for protein ligand docking. *Curr Protein Pept Sci*. 2006;7(5):407-20. doi: [10.2174/138920306778559395](https://doi.org/10.2174/138920306778559395), PMID 17073693.
- Friesner RA, Murphy RB, Repasky MP, Frye LL, Greenwood JR, Halgren TA. Extra precision glide: docking and scoring incorporating a model of hydrophobic enclosure for protein ligand complexes. *J Med Chem*. 2006;49(21):6177-96. doi: [10.1021/jm051256o](https://doi.org/10.1021/jm051256o), PMID 17034125.
- Godschalk F, Genheden S, Soderhjelm P, Ryde U. Comparison of MM/GBSA calculations based on explicit and implicit solvent simulations. *Phys Chem Chem Phys*. 2013;15(20):7731-9. doi: [10.1039/c3cp00116d](https://doi.org/10.1039/c3cp00116d), PMID 23595060.
- Allegra M, Tutone M, Tesoriere L, Attanzio A, Culetta G, Almerico AM. Evaluation of the IKK $\beta$  binding of indicaxanthin by induced fit docking binding pose metadynamics and molecular dynamics. *Front Pharmacol*. 2021;12:701568. doi: [10.3389/fphar.2021.701568](https://doi.org/10.3389/fphar.2021.701568), PMID 34566634.



29. Mishra R, Patel H, Alanazi S, Kilroy MK, Garrett JT. PI3K inhibitors in cancer: clinical implications and adverse effects. *Int J Mol Sci.* 2021;22(7):3464. doi: [10.3390/ijms22073464](https://doi.org/10.3390/ijms22073464), PMID [33801659](https://pubmed.ncbi.nlm.nih.gov/33801659/).
30. Pascual J, Turner NC. Targeting the PI3-kinase pathway in triple-negative breast cancer. *Ann Oncol.* 2019;30(7):1051-60. doi: [10.1093/annonc/mdz133](https://doi.org/10.1093/annonc/mdz133), PMID [31050709](https://pubmed.ncbi.nlm.nih.gov/31050709/).
31. Halder D, Das S, Joseph A, Jeyaprakash RS. Molecular docking and dynamics approach to in silico drug repurposing for inflammatory bowels disease by targeting TNF alpha. *J Biomol Struct Dyn.* 2023;41(8):3462-75. doi: [10.1080/07391102.2022.2050948](https://doi.org/10.1080/07391102.2022.2050948), PMID [35285757](https://pubmed.ncbi.nlm.nih.gov/35285757/).
32. Karami A, Fakhri S, Kooshki L, Khan H. Polydatin: pharmacological mechanisms therapeutic targets biological activities and health benefits. *Molecules.* 2022;27(19):6474. doi: [10.3390/molecules27196474](https://doi.org/10.3390/molecules27196474), PMID [36235012](https://pubmed.ncbi.nlm.nih.gov/36235012/).
33. Cheng H, Orr ST, Bailey S, Brooun A, Chen P, Deal JG. Structure-based drug design and synthesis of PI3K $\alpha$ -selective inhibitor (PF-06843195). *J Med Chem.* 2021;64(1):644-61. doi: [10.1021/acs.jmedchem.0c01652](https://doi.org/10.1021/acs.jmedchem.0c01652), PMID [33356246](https://pubmed.ncbi.nlm.nih.gov/33356246/).
34. Hanan EJ, Braun MG, Heald RA, Macleod C, Chan C, Clausen S. Discovery of GDC-0077 (Inavolisib) a highly selective inhibitor and degrader of mutant PI3K $\alpha$ . *J Med Chem.* 2022;65(24):16589-621. doi: [10.1021/acs.jmedchem.2c01422](https://doi.org/10.1021/acs.jmedchem.2c01422), PMID [36455032](https://pubmed.ncbi.nlm.nih.gov/36455032/).
35. Stein M, Borovik R, Robinson E. Mitoxantrone as second line single agent in metastatic breast cancer. *Oncology.* 1991;48(4):265-9. doi: [10.1159/000226940](https://doi.org/10.1159/000226940), PMID [1891166](https://pubmed.ncbi.nlm.nih.gov/1891166/).
36. Wang H, Wang Y, Li C, Wang H, Geng X, Hu B. Structural basis for tailor-made selective PI3K  $\alpha/\beta$  inhibitors: a computational perspective. *New J Chem.* 2021;45(1):373-82. doi: [10.1039/D0NJ04216A](https://doi.org/10.1039/D0NJ04216A).
37. Bhaskar BV, Rammohan A, Babu TM, Zheng GY, Chen W, Rajendra W. Molecular insight into isoform-specific inhibition of PI3K- $\alpha$  and PKC- $\eta$  with dietary agents through an ensemble pharmacophore and docking studies. *Sci Rep.* 2021;11(1):12150. doi: [10.1038/s41598-021-90287-3](https://doi.org/10.1038/s41598-021-90287-3), PMID [34108504](https://pubmed.ncbi.nlm.nih.gov/34108504/).